Geol. Mag. **149** (*4*), *2012, pp. 590–605. © Cambridge University Press 2011*
doi:10.1017/S0016756811000872

Parental magma composition of the syntectonic Dawros Peridotite chromitites, NW Connemara, Ireland

E. HUNT*†, B. O'DRISCOLL* & J. S. DALY‡

*School of Physical and Geographical Sciences, Keele University, Keele, UK
‡UCD School of Geological Sciences, University College Dublin, Belfield, Dublin 4, Ireland

(*Received* 12 February 2011; *accepted* 27 May 2011; *first published online* 14 October 2011)

Abstract – Chromium-spinels have been widely used as petrogenetic indicators to infer parent melt compositions and the tectonic setting of their formation. This study integrates petrographic, quantitative textural and geochemical analyses of Cr-spinel seams within the Dawros Peridotite, NW Connemara, Ireland to determine the composition of their parental magmas. Calculation of Cr no. (Cr/(Cr + Al)) (0.50–0.77) values and TiO_2 (0.18–0.36 wt %) contents of the Cr-spinel seams, coupled with an estimation of the Al_2O_3 and TiO_2 contents (~11.86 wt % and ~0.39 wt %, respectively) of their parental melts, indicates that they probably formed from boninitic melts sourced from a highly depleted mantle. This implies that the Cr-spinel seams formed in a supra-subduction zone undergoing high degrees of partial melting. The Cr-spinel data support tectonic models for the formation of the Dawros Peridotite (and Connemara Metagabbro-Gneiss Complex) during island arc collision, immediately prior to Grampian orogenesis at ~470 Ma. The occurrence of the Dawros chromitite seams at the approximate transition between the lower harzburgite sequence and the upper lherzolite sequence bears marked similarities to the positions of such seams in larger anorogenic layered mafic-ultramafic intrusions, and implies that the Dawros Peridotite behaved as an open-system magma chamber.

Keywords: Cr-spinel, Dawros Peridotite, island arc, boninite, melt–rock interaction.

1. Introduction

Chromitites (≥60 % modal Cr-spinel) have had widespread use as petrogenetic indicators for inferring their parent magma compositions in both layered mafic-ultramafic intrusions and in the lower mantle portions of some ophiolites (cf. Irvine, 1965, 1967; Rollinson, Appel & Frei, 2002). Of particular importance to such discriminatory studies is the Cr no. parameter (Cr/(Cr + Al)); the Cr^{3+} and Al^{3+} contents of Cr-spinel have been used to infer parental magma composition and degree of mantle melting in a wide variety of tectonic settings (Zhou & Robinson, 1997; Barnes & Roeder, 2001; Kamenetsky, Crawford & Meffre, 2001; Rollinson, Appel & Frei, 2002; Uysal *et al*. 2009; Marchesi *et al*. 2011). Broad fields on plots of Cr no. v. Fe no. (Fe^{2+}/(Fe^{2+} + Mg)) and Cr no. v. TiO_2 have been established to distinguish between formation from mid-ocean ridge basalts (MORB), boninites, komatiites and ocean island basalts; and more broadly, between the two principal modes of natural occurrence of chromitite: stratiform seams in layered intrusions and podiform seams in ophiolite settings (Zhou & Robinson, 1997; Barnes & Roeder, 2001; Kamenetsky, Crawford & Meffre, 2001; Lord *et al*. 2004). The petrogenesis of chromitite seams in both layered intrusions and in ophiolites is a long-standing problem in petrological studies of such rocks. Traditionally invoked mechanisms of formation in both settings involve the crystallization of Cr-spinel after magma mixing, followed by gravitational settling of the crystals to form stratiform seams (Irvine, 1965, 1967, 1977). Chromitite seams dominantly occur in shallowly-emplaced intra-cratonic open-system layered mafic intrusions, e.g. the Bushveld Complex (Mondal & Mathez, 2007) and the Rum Layered Suite (O'Driscoll *et al*. 2010) and in supra-subduction zone mantle ophiolite sequences (Pearce, Lippard & Roberts, 1984; Melcher *et al*. 1997; Ballhaus, 1998; Kamenetsky, Crawford & Meffre, 2001; Uysal *et al*. 2009). However, their textural and geochemical characteristics are not typically reported from mid-crustal magma chambers, such as the Dawros intrusion.

The Dawros Peridotite is a ~475 Ma (Friedrich *et al*. 1999) ultramafic layered intrusion (Bennett & Gibb, 1983; Wellings, 1997, 1998; Friedrich *et al*. 1999; O'Driscoll, Powell & Reavy, 2005) in northern Connemara, western Ireland (Fig. 1), interpreted as representing the basal cumulates of a fragmented magma chamber (Kanaris-Sotiriou & Angus, 1976; Wellings, 1997). Deformation of the primary magmatic features, including the mineral layering, has been attributed to magma emplacement during orogenesis (Wellings, 1998). The apparently small size of the intrusion and locally amphibolite-facies metamorphism that occurs in its contact aureole suggest emplacement at mid-crustal levels (Wellings, 1998; O'Driscoll, Powell & Reavy, 2005). This study couples petrography and quantitative textural analyses with Cr-spinel mineral chemistry to investigate the origin of chromitite seams that occur locally in the Dawros Peridotite. It utilises the powerful petrogenetic capabilities of Cr-spinels

†Author for correspondence: ejh9@st-andrews.ac.uk

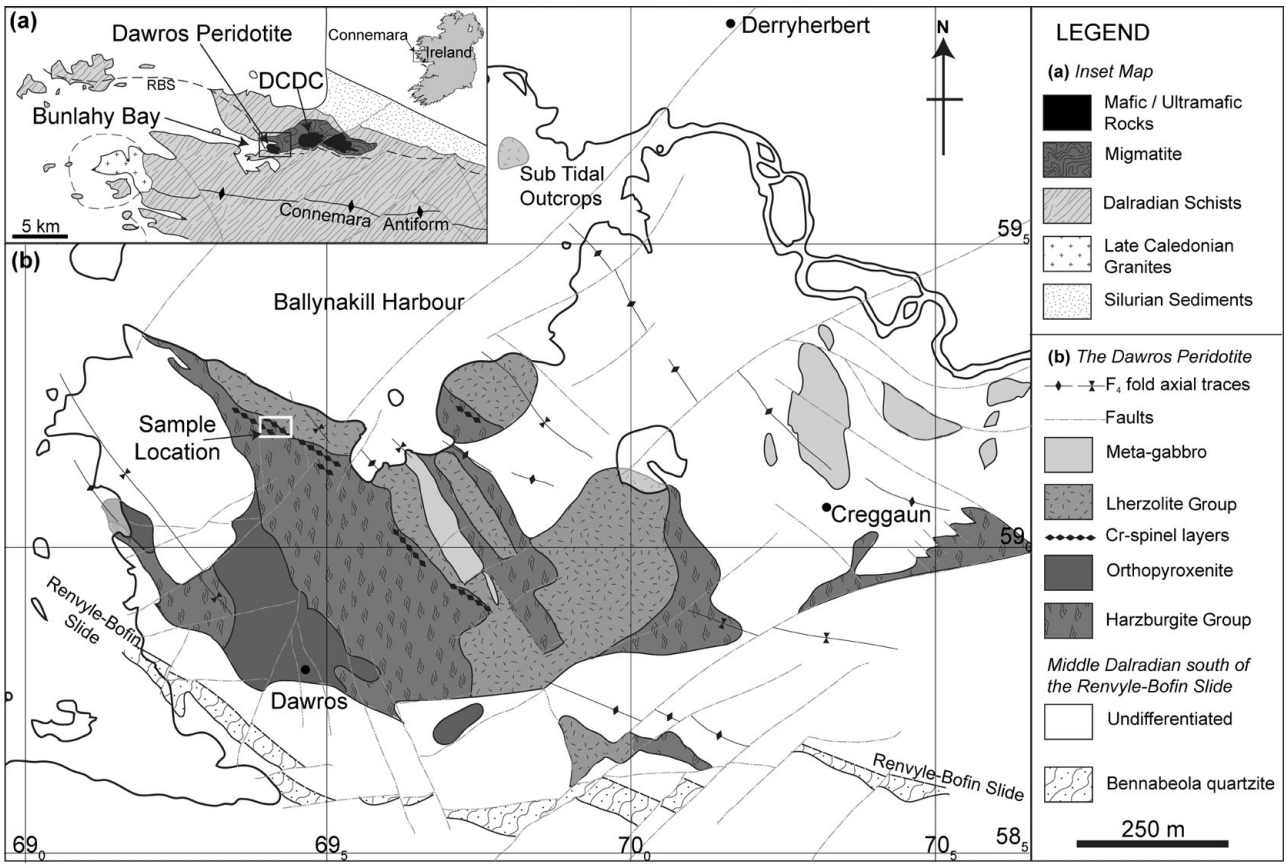

Figure 1. (a) Inset map of the northern region of Connemara, DCDC – Dawros–Currywongaun–Doughruagh Complex, RBS – Renvyle–Bofin Slide (adapted from O'Driscoll, Powell & Reavy, 2005). (b) Geological map of the Dawros Peridotite indicating the locations of the Cr-spinel horizons immediately below the boundary between the Harzburgite Group and the Lherzolite Group, with overlain Irish National Grid (adapted from Bennett & Gibb, 1983). The sample location is highlighted.

to assess their 'memory' of the parent magma from which they crystallized (Irvine, 1965; Barnes & Roeder, 2001; Kamenetsky, Crawford & Meffre, 2001). Field observations and petrography indicate that the chromitites form immediately below a horizon of major magma replenishment, supporting open-system behaviour in the Dawros magma chamber. Evidence is also preserved in the chromitite crystal size distribution (CSD) data for sub-solidus textural coarsening; an observation consistent with the behaviour of chromitite seams elsewhere (Hulbert & Von Gruenewaldt, 1985; Higgins, 2010; O'Driscoll *et al*. 2010). Cr-spinel compositions in the Dawros Peridotite seams suggest high degrees of melting of an already depleted mantle source, and support the emplacement of the Dawros Peridotite parental magmas within a supra-subduction zone, in line with magma emplacement immediately prior to island arc collision (cf. Wellings, 1998; Friedrich *et al*. 1999).

2. Geological setting

The Dawros Peridotite is an ultramafic intrusion in northern Connemara, Ireland (Fig. 1) and represents part of the Dawros–Currywongaun–Doughruagh Complex (DCDC; Ingold, 1937; Rothstein, 1957; Kanaris-Sotiriou & Angus, 1976; Bennett & Gibb, 1983; Wellings, 1997, 1998; O'Driscoll, 2005; O'Driscoll, Powell & Reavy, 2005). The DCDC is composed of a series of partially layered, foliated intrusions of varying sizes of ultrabasic (e.g. Dawros) and basic (e.g. Currywongaun) composition. These syntectonic intrusions (Bennett & Gibb, 1983; Wellings, 1997, 1998; Friedrich *et al*. 1999; O'Driscoll, Powell & Reavy, 2005) are the northern extension of the larger Connemara Metagabbro-Gneiss Complex (MGC; Leake, 1989), which crops out ∼20 km to the south (Leake & Tanner, 1994). The MGC is considered to have formed from the syntectonic emplacement of island arc magmas during the initial stages of subduction zone formation beneath Connemara (Yardley & Senior, 1982; Dewey & Shackleton, 1984; Leake, 1989; Wellings, 1998), preceding Grampian orogenesis and the development of the Irish Caledonides (Friedrich *et al*. 1999). The parental magmas to the MGC have been suggested to be hydrous tholeiites (and/or boninites) rather than the more typical high-K or calc-alkaline island arc magmas (Leake, 1989).

The Dawros Peridotite is estimated to have syntectonically intruded at mid-crustal levels (∼15 km), based on the amphibolite-facies metamorphic grade of the country rock metasediments, within the Ben Levy Grit Formation (Wellings, 1997, 1998). The Ben Levy Grit Formation comprises massive grey-green

https://doi.org/10.1017/S0016756811000872 Published online by Cambridge University Press

semi-pelites and psammites with rare volcanogenic horizons (Leake & Tanner, 1994). The formation has been assigned to the Dalradian Supergroup, but is separated from the older Argyll Group to the south by the Renvyle–Bofin Slide (Tanner & Shackleton, 1979), a low-angle orogenic structure associated with ductile deformation (Wellings, 1997, 1998).

Dalradian metasediments in the Connemara region have undergone four stages of deformation (Tanner & Shackleton, 1979) with the regional D_2 event being associated with the syntectonic intrusion of the DCDC (Wellings, 1998; O'Driscoll, Powell & Reavy, 2005). The intrusions were emplaced immediately preceding the D_3 event, with a suggested time gap of less than 0.5 Ma (Wellings, 1998). Magma emplacement during a period of ductile deformation resulted in the separation of the DCDC intrusions as lens-like bodies, along the strike of the regional foliation (Fig. 1), corresponding to a single plane of movement (Wellings, 1997). The D_3 event was regionally associated with subduction-related magmatism, arc accretion and dextral transpression, during which O'Driscoll, Powell & Reavy (2005) suggested the intrusions behaved as coherent 'mega-augen'-like bodies, while regional-scale N-verging F_3 fold nappes formed (Friedrich *et al*. 1999). During the cooling of the intrusions they were metamorphosed to amphibolite facies by the M_3 event (Kanaris-Sotiriou & Angus, 1976) and also exhibit the effects of subsequent serpentinization (Rothstein, 1957).

The Dawros Peridotite crops out over an area of 1 km^2 on the eastern side of the Ballynakill Harbour but is thought to extend northwards to where small outcrops of peridotite occur at several localities on the northern margin of Bunlahy Bay (O'Driscoll, Powell & Reavy, 2005; Fig. 1). The rocks preserve superb evidence of magmatic (mineral) layering (O'Driscoll, Powell & Reavy, 2005), which dominantly dips east. This has been taken to indicate that the intrusion youngs consistently towards the NE (Bennett & Gibb, 1983). It is composed of an ultramafic series of rocks, which have been divided into a lower harzburgite sequence and an upper lherzolite sequence (Rothstein, 1957). The harzburgite group consists of interlayered serpentinized dunite and harzburgites, with the harzburgites becoming more prevalent stratigraphically upwards (Rothstein, 1957). The lherzolite group consists of wehrlites at the transition from harzburgite, which themselves have a gradational boundary to the main lherzolites. The latter contain relict orthopyroxene and diopside crystals (Rothstein, 1957). The Cr-spinel seams occur immediately below the transition to the lherzolite group and are present within dunite bands in the harzburgite group (Fig. 1; Rothstein, 1957). The Cr-spinel seams occupy a horizon approximately 3–5 m thick and strike discontinuously across the intrusion with a general NW trend (O'Driscoll, Powell & Reavy, 2005). The seams are most abundant at the western end and particularly in the northwest of the intrusion, where well-developed chromitite occurs in seams with an average thickness of 5 cm (O'Driscoll, Powell & Reavy, 2005). The only published mineral chemical analyses to date of the Dawros Cr-spinel seams are for one Cr-spinel and two Al-spinel crystals; these indicate that the Dawros chromitite shares compositional characteristics with chromitite in both layered mafic intrusions and alpine peridotites (Rothstein, 1972).

The Dawros Peridotite lies within an upright regional F_2 fold limb and is further folded into a synform by F_3 folds (Bennett & Gibb, 1983; B. O'Driscoll, unpub. B.Sc. thesis, Univ. College Cork, 2003). Within the centre of the intrusion, and the syncline core, is a metagabbro lens, which trends NW along the line of strike of layering in the peridotite (O'Driscoll, Powell & Reavy, 2005). Two interpretations have been proposed for its origin: Bennett & Gibb (1983) regard the lens to be a later, syn-D_2 intrusion into the ultramafic cumulates, likely during the separation of the DCDC intrusions; whilst Leake (1970) suggests that the gabbro represents a continuation of the magmatic fractionation sequence in the Dawros chamber, so that its crystallization was broadly coeval with the rest of the peridotite.

3. Field observations and petrography

The chromitite was sampled at [L69415 59223] (Irish National Grid; Fig. 1), at the approximate stratigraphic transition of harzburgite upwards into wehrlite and lherzolite. Here, the Cr-spinel seams occur within serpentinized dunite layers in the harzburgite group, and range in thickness from 1 mm to 7 cm. The chromitites do not form stratiform seams, as is common in some layered mafic intrusions, but instead form elongated lenses and complex networks of chromitite schlieren (Fig. 2a–d), broadly concordant to the magmatic layering (as described by O'Driscoll, Powell & Reavy, 2005) with a typical orientation of 061/31 N. The seams show outcrop-scale evidence of having behaved both coherently and incoherently in their predominantly serpentinized dunite matrix during ductile deformation (Fig. 2). Brittle deformation has resulted in the development of serpentine-filled fractures that cut through many seams (Fig. 2b).

The chromitite seams typically comprise 90 mod. % Cr-spinel, 7 mod. % serpentine, 2 mod. % relict olivine and ~1 mod. % other oxide phases (probably titano-maghaemite and magnetite; O'Driscoll & Petronis, 2009).The Cr-spinel crystals within the seams have a larger range of crystal sizes (0.032–0.85 mm) than those disseminated in the serpentinized dunite (0.034–0.59 mm in diameter) on either side of the seams. Cr-spinel crystal sizes coarsen towards the centre of some seams (Fig 3a), an effect observed in other layered intrusions (e.g. the Stillwater Complex; Waters & Boudreau, 1996). However, coarsened angular 'fragments' of chromitite without a surrounding fine-grained margin also occur in serpentinized dunite adjacent to chromitite seams (see Fig. 3a). Cr-spinel crystals within the seams often contain spherical silicate inclusions of serpentine (Fig. 3b), taken here as

https://doi.org/10.1017/S0016756811000872 Published online by Cambridge University Press

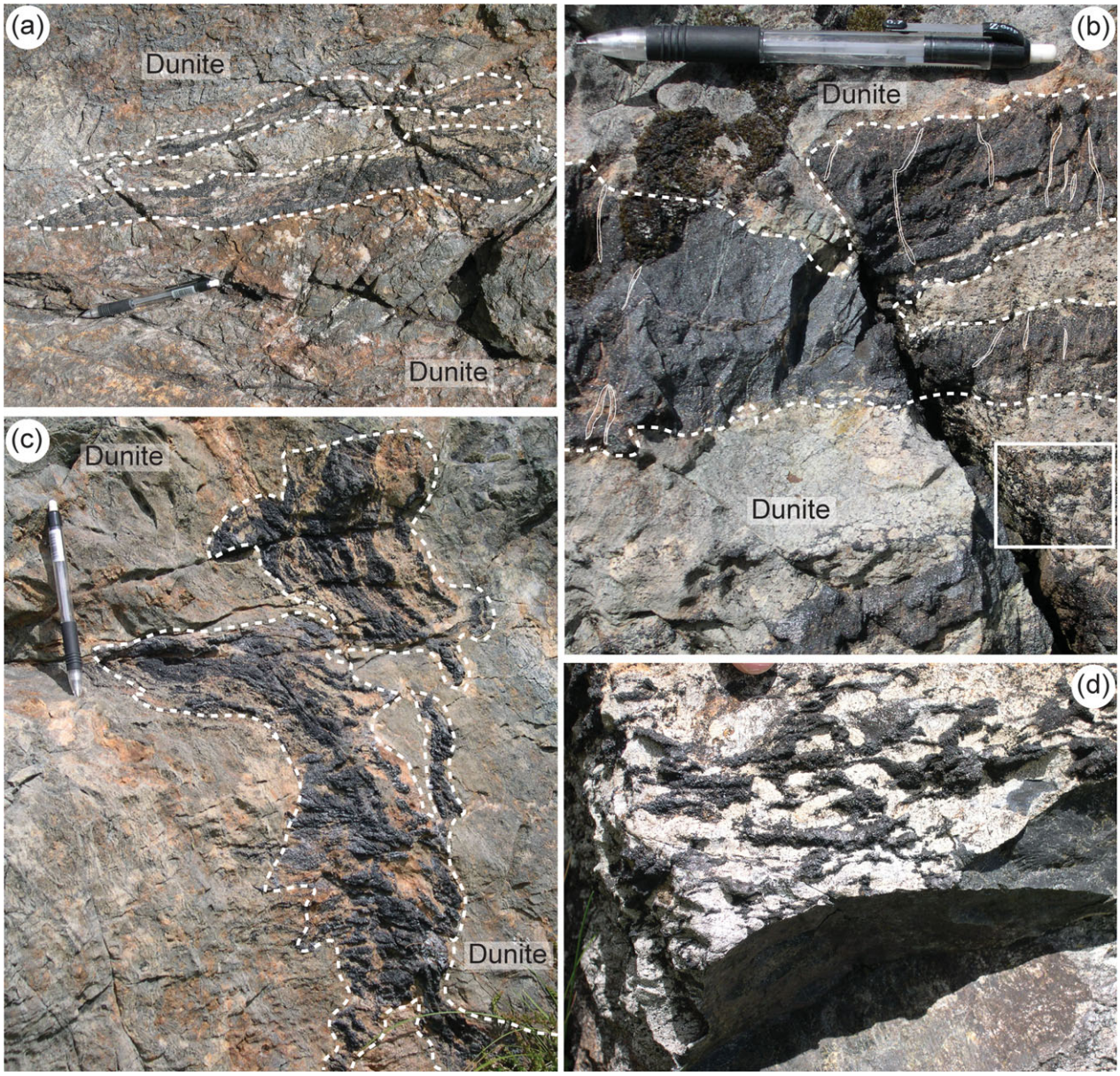

Figure 2. (Colour online) Field photographs of *in situ* Cr-spinel layers, outlined in white, in dunite. (a) Strung-out layers of Cr-spinel. (b) Fractures, outlined in white, through the Cr-spinel layers, which have been filled in by serpentinite. The box on the lower right highlights the stratigraphic location of the sampled seams. (c) Deformed seam of Cr-spinel, showing parallel alignment with the magmatic fabric. (d) Anastomosing network of Cr-spinel pods indicating incoherent deformation; fingertip at top of image for scale. The pencil shown in (a–c) is ∼15 cm long. Images (a), (c) and (d) are taken immediately adjacent to one another; the sampled Cr-spinel seams occur immediately adjacent to those highlighted in the outcrop in (b).

further evidence for localized sintering and coalescence of these crystals (cf. Hulbert & Von Gruenewaldt, 1985; O'Driscoll *et al*. 2010). Relict olivine crystals occur (Fig. 3c) in the serpentinized dunite that hosts the chromitite seams and are best preserved in close proximity to the seams. Pervasive brittle deformation of Cr-spinel crystals and seams is also evident at the millimetre scale as numerous small fractures that offset seams and some larger intra-seam crystals, predominantly with a reverse sense of movement (Fig. 3d). Magnetite and titanomaghaemite are characterized by higher reflectivity than Cr-spinel and form reticulate networks and veins in and around the relict olivine crystals and olivine pseudomorphs (Fig. 3e). The internal geometry of these veins suggests a complex serpentinization history, with multiple stages of fluid transport through the rocks (Fig. 3f). Rare sulphides, usually pyrrhotite, are present, typically moulded onto the edges of Cr-spinel crystals or as spherical inclusions within Cr-spinel. The Cr-spinel crystals are often rimmed and partially replaced along fractures by ferritchromit (Fig. 3b).

4. Analytical methods

4.a. Quantitative textural analysis

Crystal size distribution (CSD) analysis is commonly used to quantify petrographic observations and provides a measure of the number of crystals of a

https://doi.org/10.1017/S0016756811000872 Published online by Cambridge University Press

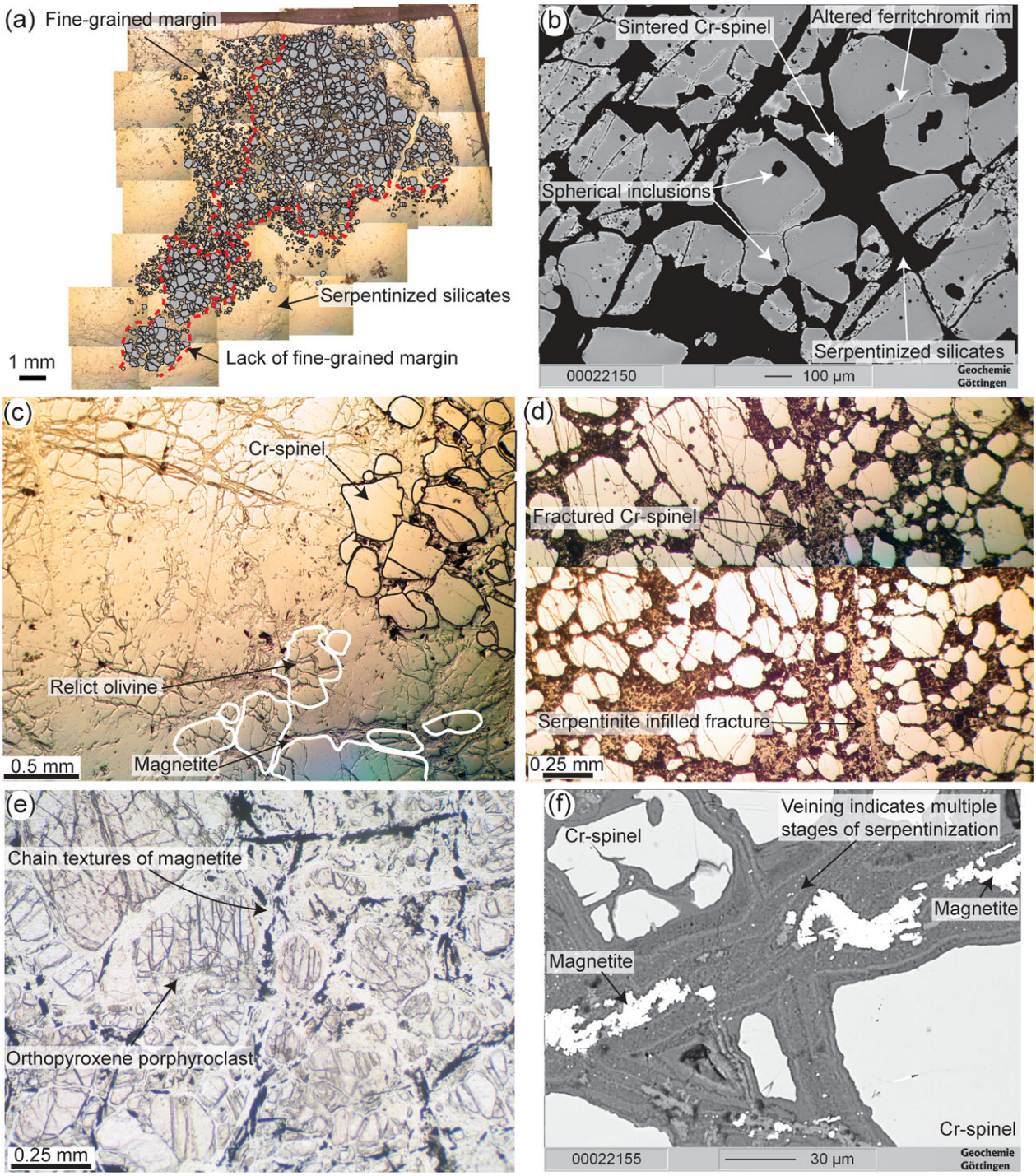

Figure 3. (Colour online) (a) Digitized thin-section image indicating coarsening of Cr-spinel crystals (highlighted) towards the centre of Seam 1. (b) BSE image of Cr-spinel crystals from Seam 2 showing spherical silicate inclusions and altered ferritchromit rims. (c) Reflected light image of relict olivine crystals in close proximity to Seam 1. (d) Reflected light image showing fracturing of Cr-spinel crystals in association with serpentinite infilled fractures through Seam 3. (e) Plane polarized transmitted light image of reticulate networks and chain textures of magnetite around the orthopyroxene and olivine porphyroclasts. (f) BSE image of serpentinite veins in Seam 1 indicating complex, multi-stage serpentinization.

mineral, per unit volume within a series of defined size intervals (Marsh, 1998; Higgins, 2006). Crystal size distribution measurements were carried out to quantify the differences in Cr-spinel textures within and without the seams, and to assess whether the pervasive brittle deformation was effective in generating new Cr-spinel grains in the seams. The data are usually plotted as population density (logarithmic number of crystals per unit volume) against crystal size (maximum length). The gradients of the resulting graphs can be useful in discriminating between different texture-forming events, with CSD plot shape changes such as kinking and curvature being related to processes such as crystal accumulation, compaction, mixing of crystal

https://doi.org/10.1017/S0016756811000872 Published online by Cambridge University Press

Table 1. CSD input and output data

Sample	Measured area (mm^2)	No. of crystals	R^2	CSD slope (mm^{-1})	Intercept (mm^{-4})	Big 'R'
Seam 1	146.70	3135	0.94	−20.0	8.60	0.89
Seam 1 Centre	145.29	1628	0.84	−15.3	7.38	0.72
Seam 1 Margin	116.30	1508	0.95	−33.2	9.28	0.54
Seam 2	85.10	1841	0.81	−21.3	8.76	0.85
Seam 3	118.70	6222	0.99	−27.6	9.99	1.13
Disseminated	131.30	581	0.97	−23.4	7.35	0.56

populations and post-nucleation coarsening caused by annealing or Ostwald ripening (Marsh, 1998; Boorman, Boudreau & Kruger, 2004; Higgins, 2006). Within this study we define textural equilibration as the extent to which the rocks evolve from the initial reaction controlled texture at the postcumulus (supra- and sub-solidus) stages (cf. Higgins, 2010). These processes include textural coarsening and sintering, due to the growth of larger grains at the expense of smaller grains, along with the coalescence of grains, resulting in a porosity reduction in the chromitite.

CSDs were calculated from thin-sections using the methods of Higgins (2000) and the program CSDCorrections v. 1.3.9.1 (Higgins, 2009). The CSD data were extracted from measurements made on digitized photomicrographs captured in reflected light (using the image analysis software ImageJ). This study has followed the method outlined in O'Driscoll *et al*. (2010) for the calculation of CSDs from reflected light images, so that the length of a square with an equal area to that of the analysed crystal was adopted as the measured crystal size parameter. This approach means that an aspect ratio of 1:1:1 and a roundness value of zero are input into the CSDCorrections software, reflecting the typically equant shape of the Cr-spinel crystals. No alignment of crystals was observed within the seams, apart from within the micro-shear zones, which were avoided. The smallest Cr-spinel crystals are easily visible in reflected light and measurable in thin-section; therefore it is inferred that the smallest grain size reported for each sample is the lower limit for that sample.

4.b. Mineral chemistry

Backscattered electron (BSE) imaging and chemical analyses of minerals were performed using the JEOL 8900 RL electron microprobe at the Department of Geochemistry, Geowissenschafliches Zentrum der Universität Göttingen. Mineral compositions for Cr-spinel and olivine were obtained with an acceleration voltage of 15 kV. Beam currents of ∼15 nA and ∼20 nA with probe diameters of 1 μm and 20 μm were used for Cr-spinel and olivine respectively. For Cr-spinel count times on peak and on background for Mg, Al, Cr, Fe and Si were 15 s and 5 s, respectively, and 30 s and 15 s, respectively, for V, Ti, Mn, Ni, and Zn. Olivine count times were 15 s on peak for Si, Na, K, Fe, Mg, Mn and 30 s on peak for Ti, Al, Ca, Ni and Cr, with backgrounds analysed for 5 s for all elements except Ni (15 s). The Fe^{3+} content was calculated from the method of Droop (1987), assuming perfect stoichiometry. However, it has been noted that the assumption of an ideal formula XY_2O_4 is erroneous in some instances (cf. Ballhaus, Berry & Green, 1991; Quintiliani, Andreozzi & Graziani, 2006), so small variations in Fe^{3+} are treated cautiously.

The Cr-spinels targeted for electron microprobe analysis were fresh, euhedral crystals; those Cr-spinels exhibiting the effects of alteration and serpentinization (e.g. ferritchromit rims) were avoided. Three (≤1.5 cm thick) chromitite seams were analysed in the area of outcrop illustrated in Figure 2b (see also Fig. 1), ∼10 cm below the bifurcating ∼7 cm thick seam at the centre of Figure 2b and located within 3–5 cm (vertically) of each other. Each of the seams is laterally discontinuous at the centimetre scale, so that they resemble stratigraphically-constrained lenses up to 30 cm long, rather than stratiform seams typical of layered mafic intrusions. The sampled seams have been arbitrarily labelled 1–3 for ease of reference. Vertical traverses taken through two of these chromitite lenses consisted of 45 and 10 spot analyses (for a thick (∼11.5 mm, Seam 3) and thin (∼3.5 mm, Seam 2) seam, respectively), to assess within-seam compositional variation. Other Cr-spinels analysed are (1) ten spot points from the centres of euhedral Cr-spinel crystals at the middle of Seam 1; (2) two intra-crystal traverses comprising 14 and 15 points, respectively, from the middle of Seam 2; (3) eight additional points analysed on Cr-spinel crystals at the margins of Cr-spinel Seam 1 and disseminated within the serpentinite groundmass near Seam 3; (4) two points from a small Cr-spinel inclusion in an olivine crystal at the margin of Seam 1. In addition, five spot analyses of fresh olivine situated close to the margin of Seam 1 were carried out in order to provide a lower estimate for the equilibration temperature of the Dawros chromitites, using the Fe–Mg exchange thermometry of Ballhaus, Berry & Green (1991).

5. Results

5.a. Quantitative textural analysis results

Crystal size distribution data are presented in Table 1 and plotted in Figure 4. The raw CSDCorrections v. 1.3.9.1 files have been placed in the supplementary materials (see online Appendix 1 at http://journals.cambridge.org/geo). Least squares regression

https://doi.org/10.1017/S0016756811000872 Published online by Cambridge University Press

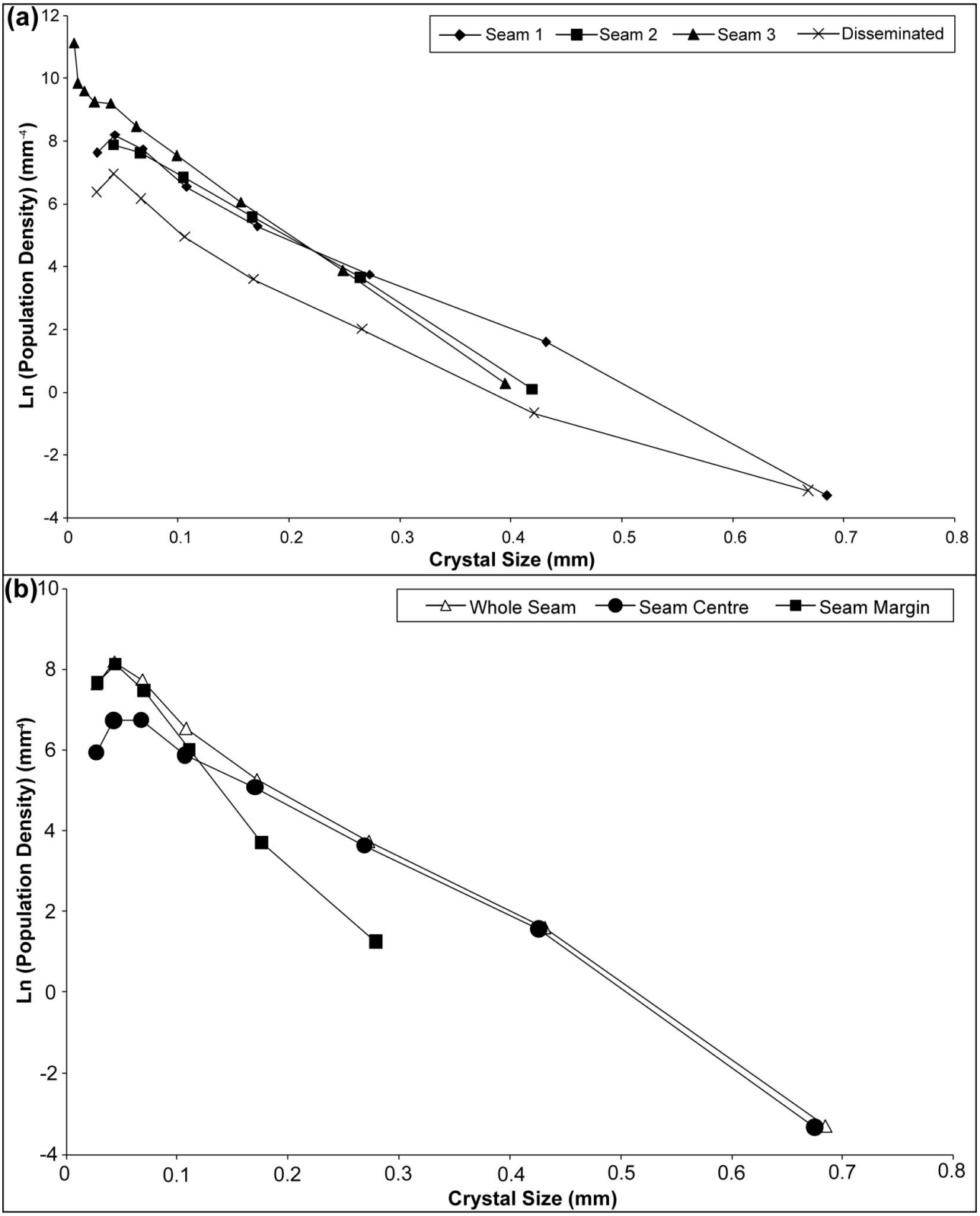

Figure 4. (a) CSD plot for seams 1 to 3 and the disseminated crystals above Seam 3. (b) CSD plot for Seam 1 from the Dawros chromitites, indicating the variation in textures, highlighted in Figure 3a, with fanning of the CSD slopes from the seam margin to the seam centre.

(R^2) analysis of the large size fractions of the CSD plots reveals good correlations (mean value of 0.92). The CSD slope values for the seams (Fig. 4a) show some intra-seam variation (-27.6 mm^{-1} to -20.0 mm^{-1}) and the disseminated crystals measured close to Seam 3 reveal a slope of -23.4 mm^{-1}; the intercept value is greater for each of the three seams (Seam 1 = 8.60 mm^{-4}, Seam 2 = 8.76 mm^{-4}, Seam 3 = 9.99 mm^{-4}) compared to that for the disseminated crystals (7.35 mm^{-4}). The shapes of the CSD curves

https://doi.org/10.1017/S0016756811000872 Published online by Cambridge University Press

Table 2. Typical Cr-spinel and relict olivine compositions for the major modes of occurrence observed in the Dawros Peridotite

Sample	SiO_2	TiO_2	Al_2O_3	Cr_2O_3	V_2O_3	FeO	Fe_2O_3	MnO	MgO	ZnO	NiO	wt % total
Cr-spinel Seam 1	0.01	0.30	17.22	41.17	0.19	23.80	9.57	0.39	6.79	0.11	0.12	99.68
Cr-spinel Seam 2	0.01	0.34	21.33	35.20	0.18	26.65	9.51	0.45	5.21	0.14	0.13	99.14
Cr-spinel Seam 3	0.01	0.24	11.87	49.04	0.22	22.62	8.21	0.38	7.08	0.07	0.10	99.84
Cr-spinel near boundary of Seam 1	0.01	0.34	17.55	39.72	0.23	23.86	10.24	0.36	6.80	0.02	0.10	99.23
Cr-spinel inclusions within olivine	0.01	0.33	19.19	39.42	0.24	23.43	9.10	0.34	7.30	0.09	0.10	99.54
Cr-spinel within serpentinite matrix	0.05	1.70	4.72	35.57	0.55	28.21	22.29	0.47	3.13	0.07	0.19	98.94
Olivine	39.69	0.00	0.00	0.03	–	10.86	–	0.18	48.14	–	0.30	99.28

Iron content for olivine data reported as combined FeO and Fe_2O_3.

are more complex at small crystal sizes, with a general humped, concave-downwards shape; apart from Seam 3, which shows a humped concave-upwards shape, indicating greater numbers of the smallest crystals.

Separating the CSD plot for Seam 1 into its constituent parts (seam margin and centre; Fig. 4b) illustrates the aforementioned coarsening of Cr-spinel crystals at the centre of the seam (cf. Marsh, 1998), with the fanning of the curves indicating an increase in maximum crystal diameter from 0.27 mm (min) at the margins of the seam to 0.66 mm (max) in the centre of the seam.

5.b. Mineral chemical results

The full Dawros mineral chemical dataset is tabulated in the supplementary materials (see online Appendix 2 at http://journals.cambridge.org/geo). Table 2 indicates the typical compositions of the Cr-spinel seam components and olivine crystals analysed and summary plots are also presented in Figure 5a and 5b. The data reveal that the composition of Cr-spinel in the seams is Cr-rich and Al-poor, with a Cr no. range of 0.53–0.77 for the Cr-spinel at the centres of the seams (Seam 1 = 0.62–0.66, Seam 2 = 0.53–0.60, Seam 3 = 0.70–0.77). TiO_2 contents of these Cr-spinels are also very low with a range of 0.18–0.34 wt % (Seam 1 = 0.27–0.32 wt %, Seam 2 = 0.23–0.34 wt %, Seam 3 = 0.18–0.27 wt %). Towards the margins of the seams, Cr no. and TiO_2 ranges are 0.50–0.79 (Seam 2 = 0.50–0.56, Seam 3 = 0.68–0.79) and 0.19–0.36 wt % (Seam 2 = 0.29–0.36, Seam 3 = 0.19–0.28), respectively. Ranges for Mg no. ($Mg/(Mg + Fe^{2+})$) for Cr-spinels from the centres and margins of the seams are 0.18–0.35 (Seam 1 = 0.25–0.27, Seam 2 = 0.18–0.21, Seam 3 = 0.27–0.35) and 0.18–0.31 (Seam 2 = 0.18–0.22, Seam 3 = 0.27–0.31), respectively. Cr-spinel crystals at the margins of the seams (Fig. 6) frequently display evidence of compositional zoning, with a thin rim of ferritchromit surrounding the Cr-spinel crystals. The Cr-spinel crystals in the serpentinite matrix have markedly different compositions (values of Cr no. = 0.84–0.88, TiO_2 = 0.74–2.18 wt %, Fe no. = 0.88–0.91, Mg no. = 0.09–0.12). Ternary Fe^{3+}–Cr–Al plots (Fig. 5c) suggest the data follow the Cr–Al trend from Barnes & Roeder (2001), indicating that $Fe^{2+}/(Fe^{2+} + Mg)$ increases with increasing $Cr/(Cr + Al)$, corroborated by Figure 7a, although the overall Mg no. content of the Cr-spinel seams is low (Fig. 8). Cr-spinel equilibration temperatures were calculated using the olivine-spinel Fe–Mg exchange thermometer of Ballhaus, Berry & Green (1991), revealing a closure temperature of ~644 °C.

6. Discussion

6.a. Magma chamber setting of the Dawros chromitites

A number of petrogenetic models for chromitite seam formation in layered intrusions have been invoked, most of which are based on the original work of Irvine (1965, 1967, 1977), involving the 'switching-off' of silicate crystallization in a hybrid magma and resultant crystallization of Cr-spinel alone due to the curvature of the olivine-spinel cotectic on the Mg_2SiO_4–$CaMgSi_2O_6$–$CaAl_2Si_2O_8$–$MgCr_2O_4$–SiO_2 join. Adaptations of this model have proposed that chromitites form after the injection of a hotter, chemically primitive melt, which partially assimilates the crystal mush, leading to the *in situ* crystallization of Cr-spinel crystals (Rum Layered Suite; O'Driscoll *et al.* 2010) or through crystal settling from emplacement of new magma batches with entrained cargoes of Cr-spinel crystals (Bushveld Complex; Mondal & Mathez, 2007). It is important to note that chromitite seams in layered intrusions are associated exclusively with open-system magma chambers, i.e. those that have been constructed by the addition of batches of new melt throughout their evolution. The pattern of outcrop of the Dawros chromitites along a NW–SE strike parallel to magmatic layering suggests a stratiform mode of occurrence, and their presence immediately below a major lithological change (harzburgites to lherzolite) in the Dawros 'stratigraphy' is reminiscent of chromitite seams in other layered mafic intrusions, in which Cr-spinel seams occur below magma replenishment horizons, implying that the Dawros chamber also experienced open-system behaviour, as suggested by other workers (Leake, 1958; Bremner & Leake, 1980). Chromitites from layered mafic intrusions tend to show a strong Fe–Ti trend, due to fractionation of magma within the crust and the reaction of the Cr-spinels with evolving interstitial fluids (Barnes & Roeder, 2001). However, the chemical characteristics of chromitite seams from mid-crustal magma chambers have not been extensively documented. The mineral

https://doi.org/10.1017/S0016756811000872 Published online by Cambridge University Press

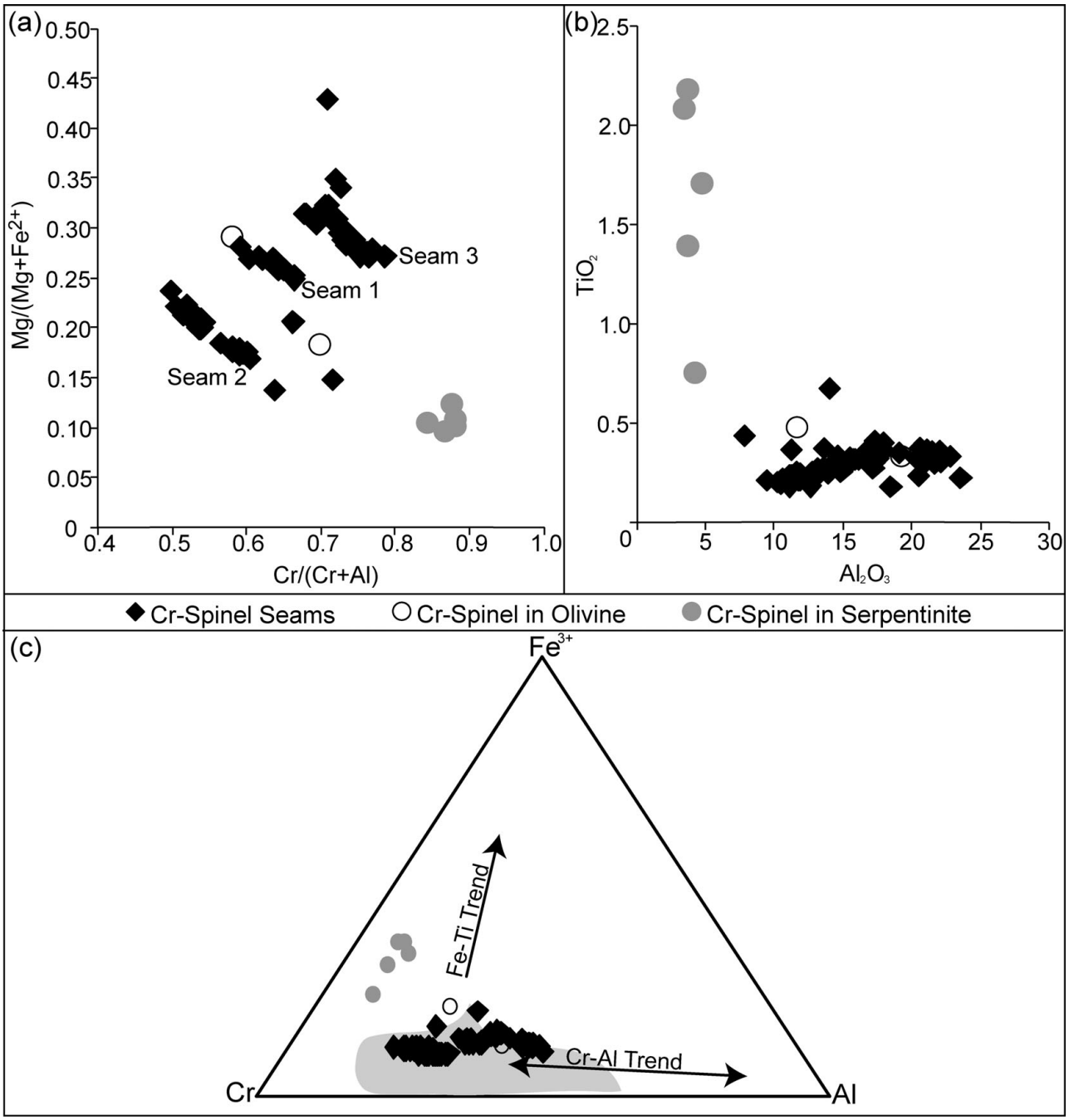

Figure 5. (a) Plot of Mg no. v. Cr no. (b) Plot of TiO_2 v. Al_2O_3. In both (a) and (b), data points outside the main fields defined by the seam compositions represent alteration to ferritchromit at crystal rims. Note the difference in composition between the Cr-spinel seams and the Cr-spinel disseminated within the serpentinite matrix. (c) Ternary diagram indicating the bulk of the data follow the Cr–Al trend, with the shaded field representing chromitites from ocean floor peridotites (dredged or cored). Fields and trends are taken from Barnes & Roeder (2001).

chemistry of the Cr-spinels crystallized at Dawros is not characteristic of typical layered intrusion chromitites, particularly with respect to Cr no., which is relatively high, and TiO_2 content, which is considerably lower than would be expected (Fig. 7; Barnes & Roeder, 2001).

The pervasive serpentinization of the silicate mineralogy makes it difficult to describe primary magmatic textures, so evaluation of the exact mechanism for chromitite seam formation is difficult. However, the presence of the chromitites immediately below what is suggested to be a magma replenishment horizon would seem to suggest that either the resident and the new magma mixed to force crystallization of large amounts of Cr-spinel (cf. Irvine, 1977), or interaction (downward infiltration and assimilation) of the hotter replenishing magma with the crystal mush floor may have triggered chromitite seam formation, as has recently been suggested for chromitites in the Rum Layered Suite (O'Driscoll *et al*. 2010), forming the Cr-spinel seams below the magma replenishment horizon. The latter model bears more similarities to

https://doi.org/10.1017/S0016756811000872 Published online by Cambridge University Press

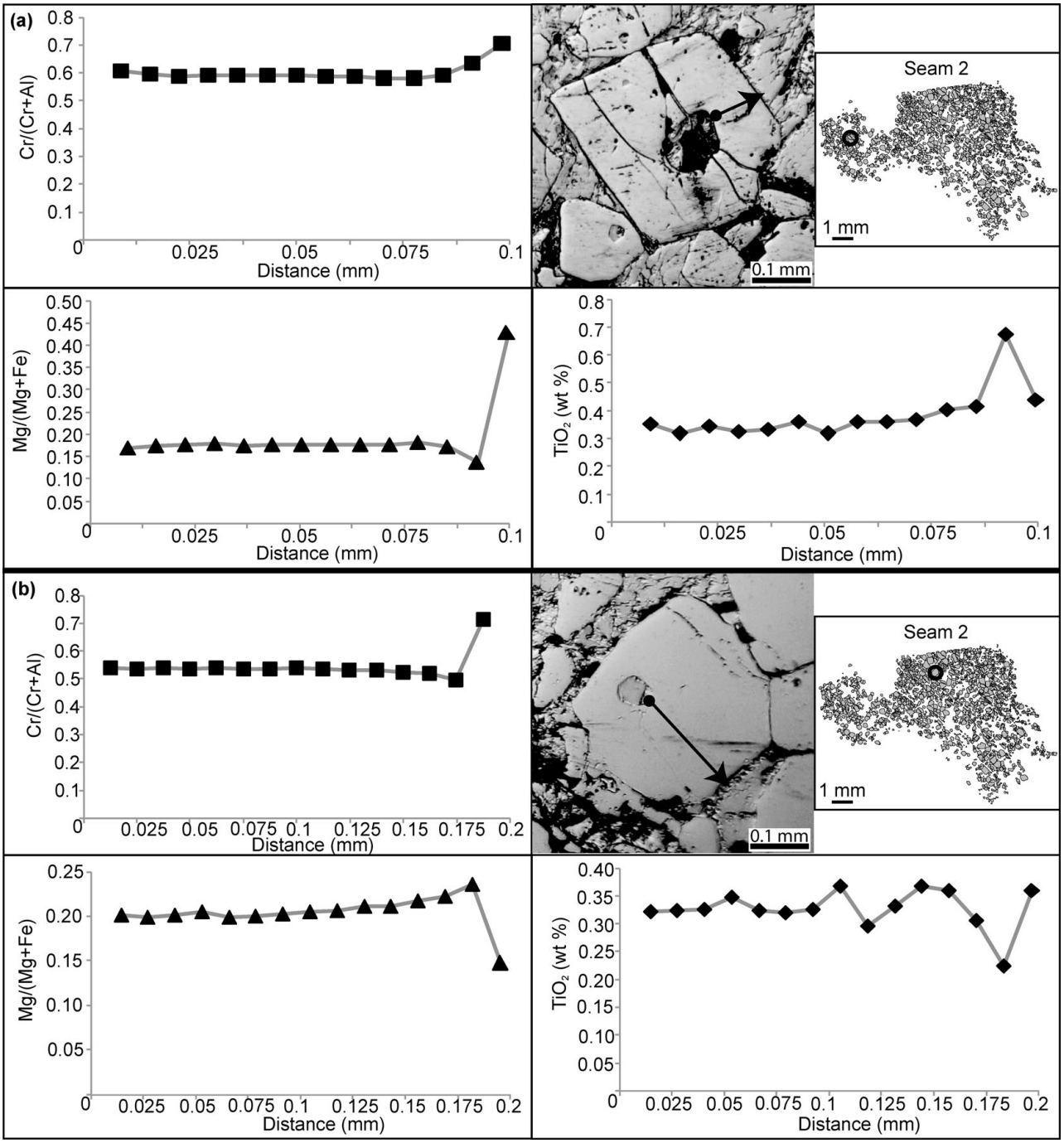

Figure 6. (a, b) Compositional variations in the Cr-spinel crystals, from core to rim. Top right panel in each indicates location of traverse across each crystal and the location of the crystal within the seam. Each traverse is taken from the margin of the silicate (orthopyroxene) inclusion to the Cr-spinel crystal margin with serpentinite.

the melt–rock interaction process often invoked for the crystallization of ophiolite chromitites (Kelemen *et al*. 1995, 1997; Zhou *et al*. 1996; Zhou & Robinson, 1997; Büchl, Brügmann & Batanova, 2004). Melt percolation in lherzolitic mantle peridotite results in clinopyroxene dissolution and incongruent melting of orthopyroxene, resulting in olivine precipitation from the melt (Kelemen *et al*. 1997). If partial melting proceeds to the point where only olivine-rich residues remain, Cr behaves incompatibly, allowing large amounts of Cr to be mobilized. Consequent supersaturation of the melt in Cr-spinel leads to the 'switching-off' of olivine crystallization, instead resulting in the precipitation of podiform chromitites (Büchl, Brügmann & Batanova, 2004). It is important to note in this light that the Dawros chromitites occur within dunite layers and also rarely occur as orbicular nodules within subhedral olivine crystals, which closely resemble some podiform chromitite deposits (Rothstein, 1972), suggesting a similar petrogenetic model to that for ophiolite chromitites outlined above.

The above arguments imply that the DCDC magma chamber was filled by several magma pulses, rather than a simple one-stage filling episode that resulted in

https://doi.org/10.1017/S0016756811000872 Published online by Cambridge University Press

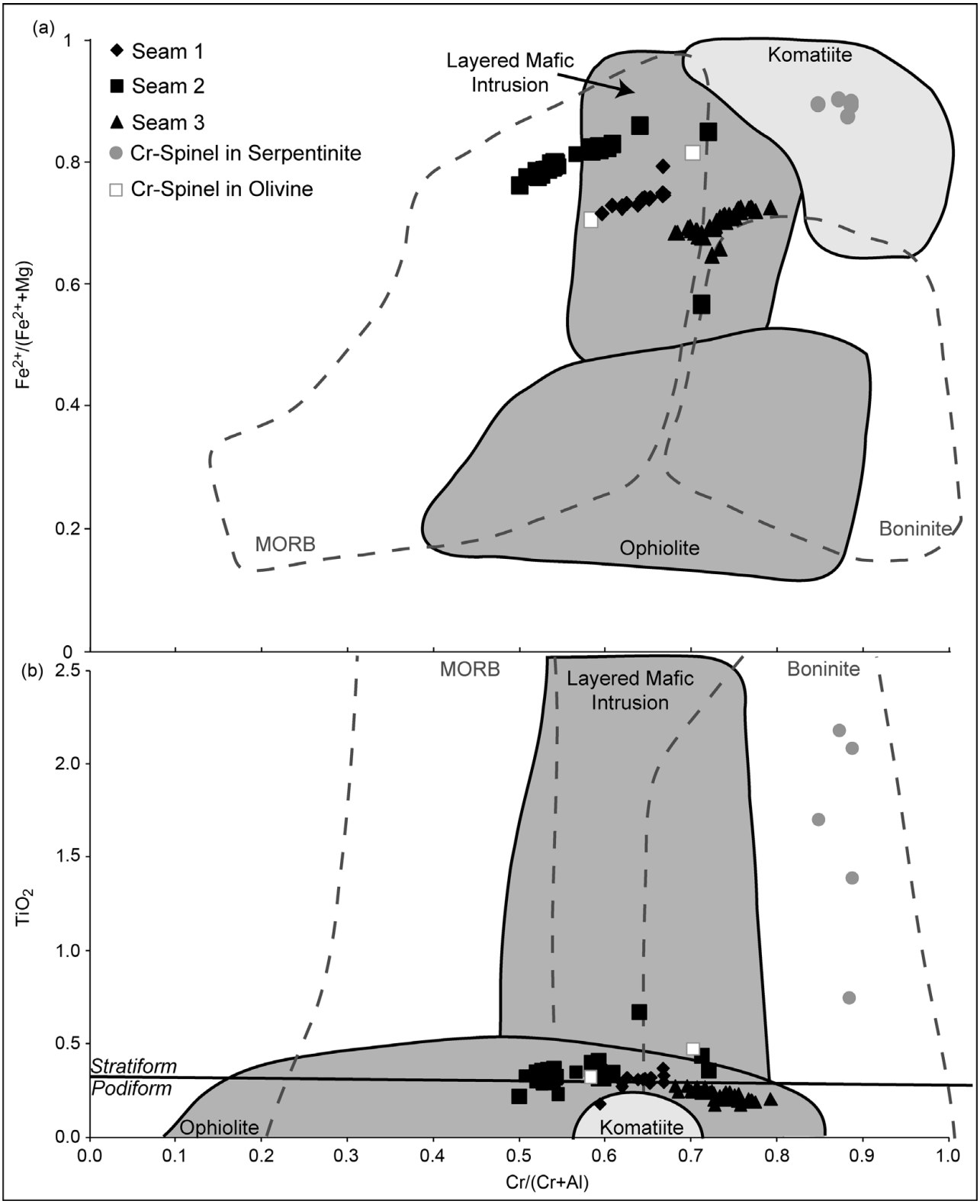

Figure 7. (a) Plot of Fe^{2+} no. v. Cr no. of Cr-spinels from the Dawros Peridotite compared to fields of typical Cr-spinel compositions formed within layered mafic intrusions, komatiites and ophiolites (shaded fields). Typical MORB and boninite compositions are outlined by dashed lines. (b) TiO_2 v. Cr no. of Cr-spinel from the Dawros Peridotite compared to fields of typical Cr-spinel compositions, as above. Fields plotted from Bonavia, Diella & Farrario (1998) and Barnes & Roeder (2001).

the accumulation of the Dawros cumulates at the base of the magma chamber (Kanaris-Sotiriou & Angus, 1976). This is in agreement with previous stratigraphical and petrological studies of the complexes related to the DCDC, e.g. the Cashel-Lough Wheelaun intrusion and the Roundstone Ultrabasic Complex in South Connemara, where numerous ultramafic xenoliths within the gabbroic intrusions have been used to infer multiple replenishment events (cf. Leake, 1958; Bremner & Leake, 1980). The subtly different compositions of

https://doi.org/10.1017/S0016756811000872 Published online by Cambridge University Press

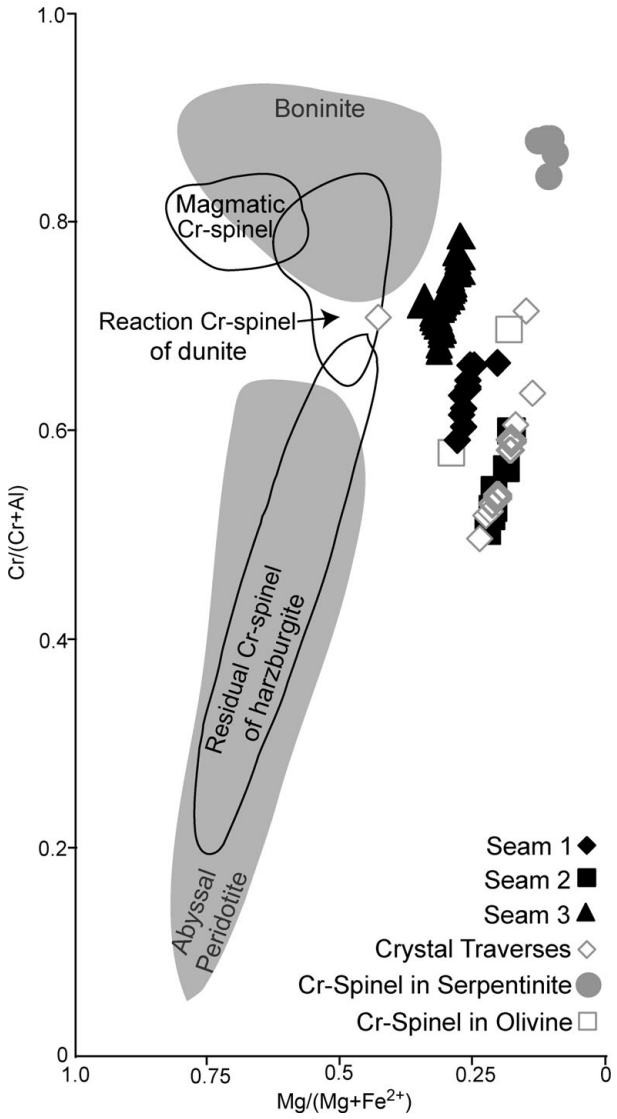

Figure 8. Plot of Cr no. v. Mg no. Note the Mg-poor composition of the Dawros Cr-spinels. Fields from Zhou *et al*. (1996).

Cr-spinel from the different seams may reflect slightly differing parental magma compositions for each of the seams, likely indicating different degrees of melt–rock interaction during the formation of each of the individual seams (Barnes, 1998). Such compositional variations in chromitite seam composition in individual intrusions have been observed elsewhere, notably within the Bushveld Complex (Naldrett *et al*. 2009) and the Rum Layered Suite (O'Driscoll *et al*. 2009), as well as within podiform chromitites in ophiolites (e.g. the Shetland ophiolite chromitites; O'Driscoll, unpub. data) and have also been attributed to slight variations in parental melt composition during individual seam formation.

Whatever the catalyst for chromitite seam formation, it is clear that Cr-spinel crystals in the seams have texturally coarsened in a manner similar to that observed in other layered intrusion settings. Calculation of thermal equilibration temperatures using olivine-spinel Fe–Mg exchange thermometry (Ballhaus, Berry & Green, 1991) yields closure temperatures of ~644 °C. This suggests that the coalescence of the Cr-spinel crystals may have occurred down to temperatures typical of the final stages of solidification of layered mafic intrusions, although the effects of sub-solidus coarsening are also likely to have played a part. The previously described curvature and fanning of the CSD slopes indicates that processes of coalescence and sintering have affected the crystals, resulting in an increase in the volume of larger crystals at the expense of smaller crystals. The effects of the regional deformation and metamorphism during the cooling of the DCDC complex are not believed to have significantly enhanced textural equilibration, as petrographic evidence reveals coarser-grained fragments of chromitite that lack a fine-grained margin distributed throughout the serpentinite (Fig. 3a). This suggests that textural coarsening occurred before the regional metamorphism and ductile deformation. Serpentinization resulted in the formation of ferritchromit rims (Fig. 3b) on the margins of Cr-spinel crystals and along fracture networks through the crystals. The intact reticulate networks of magnetite in the serpentinite groundmass occur within veins that show no obvious evidence for deformation, indicating that the serpentinization was a low-temperature event that occurred subsequent to deformation (Fig. 3e, f).

6.b. Tectonic setting of the Dawros Peridotite parent magmas

It is clear from this work that the Dawros chromitites have compositional and textural affinities with both layered mafic intrusions and ophiolite complexes. Chromitite seams are present within ophiolite complexes as podiform chromitites, which occur as irregular, cross-cutting to stratabound bodies (Ballhaus, 1998). The chromitites are usually situated close to the petrologic Moho (Zhou *et al*. 1998) and their textures range from nodular and orbicular to massive and disseminated. The ubiquitous occurrence of these podiform seams within dunite layers and lenses in upper mantle harzburgitic host-rock has increasingly led to the interpretation that ophiolite chromitites form as channels of focused melt flow and the high degree of melt–rock interaction that occurs within these channels (Kelemen *et al*. 1995, 1997; Zhou *et al*. 1996, 1998; Zhou & Robinson, 1997; Ballhaus, 1998). As podiform chromitites are predominantly found within the mantle portions of ophiolites within supra-subduction zone settings, it has been suggested that the interaction of volatile-rich melts from the subducting slab lowers the solidus temperature of the overlying mantle wedge and the resultant high degree (~25 %) of partial mantle melting is critical to chromitite formation in these settings (Pearce, Lippard & Roberts, 1984; Zhou & Robinson, 1997; Zhou *et al*. 2001; Ahmed *et al*. 2009; Uysal *et al*. 2009). Cr-spinel composition (specifically Cr no. and TiO_2 content) has been used to define two compositional end-members for the magmas that produce ophiolite chromitites, a high Al–low Cr variety (Cr no. = 49–55, TiO_2 = 0.20–0.29 wt %) and a high

https://doi.org/10.1017/S0016756811000872 Published online by Cambridge University Press

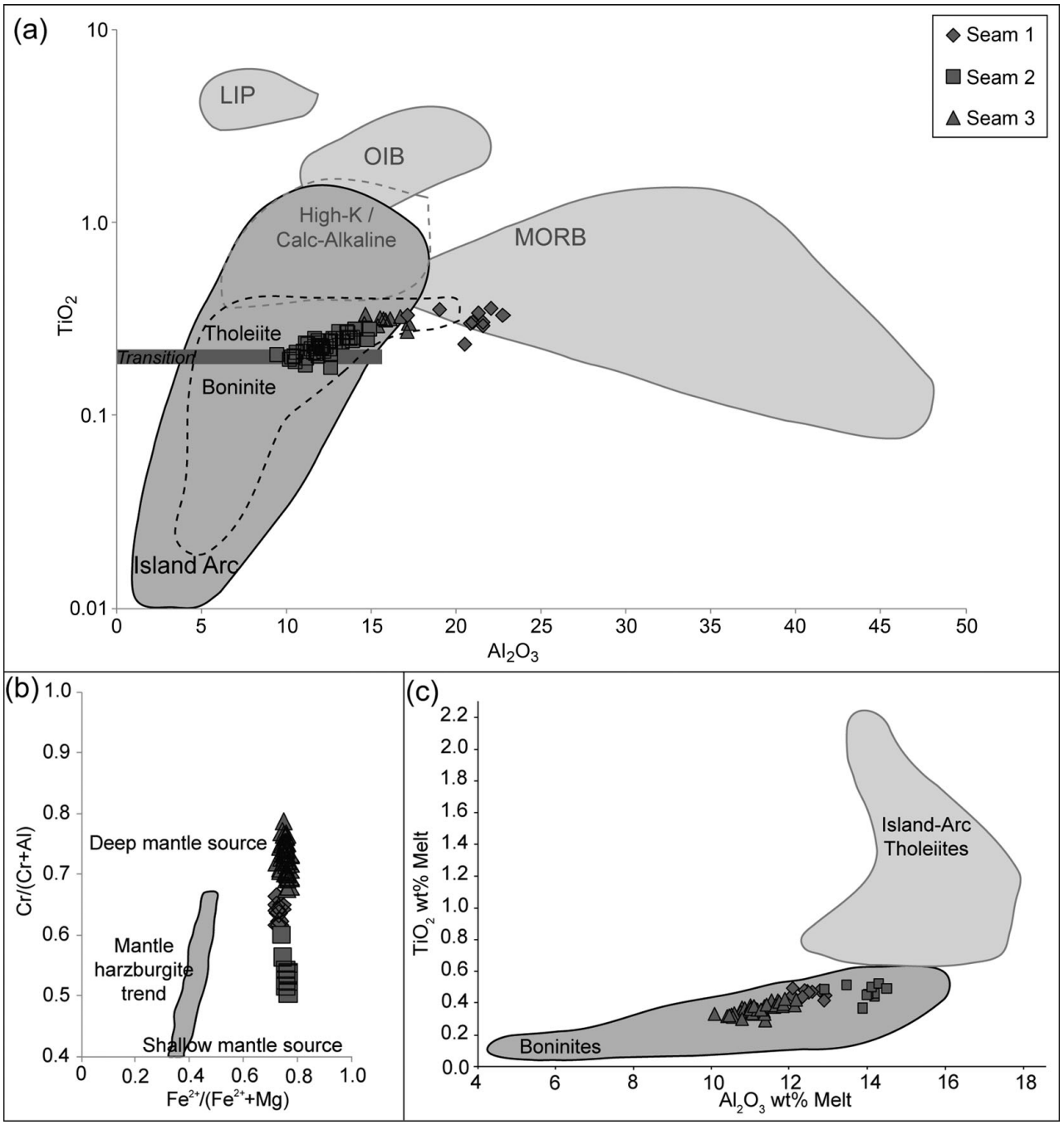

Figure 9. (a) TiO_2 v. Al_2O_3 discrimination diagram indicating that the Dawros Cr-spinel seams correspond to an island-arc tectonic setting, producing boninitic or tholeiitic magmas (fields from Kamenetsky, Crawford & Meffre, 2001; transition zone marks change from island arc tholeiites to island arc boninites, from Page & Barnes, 2009). (b) Classification diagram for constraining the source magma depth, indicating a deep mantle source for the Dawros Peridotite parent melts, after Rollinson (2008). (c) TiO_2 wt % melt v. Al_2O_3 wt % melt discrimination diagram for parental magma composition also suggesting the Dawros Cr-spinel seams formed from boninitic composition magmas (fields plotted from Page & Barnes, 2009). Only data from Cr-spinel crystal cores have been plotted to avoid affects from the altered crystal rims.

Cr–low Al (Cr no. = 71–79, TiO_2 = 0.09–0.15 wt %) variety (Zhou *et al*. 1998). Ophiolite chromitites are commonly associated with strong Cr–Al trends and are generally poor in Fe^{3+} and Ti, although high-Ti Cr-spinels may occur within ophiolite magma chambers (Barnes & Roeder, 2001). The high-Al Cr-spinel chromitites are rare, and are attributed to magmas that formed from low degrees of dry partial melting at fast-spreading mid-ocean ridge settings (Zhou & Robinson, 1997; Ahmed *et al*. 2009; Uysal *et al*. 2009). The high-Cr variety are by far the most common, and are attributed to formation from magmas generated by high degrees of hydrous partial melting of an already depleted mantle source above active subduction zones (Zhou & Robinson, 1997; Rollinson, 2008; Uysal *et al*. 2009).

The DCDC complex has been interpreted as the northern extension of the MGC (Leake & Tanner, 1994; Wellings, 1998), cropping out on the opposite (northern) limb of the major D_4 Connemara Antiform.

https://doi.org/10.1017/S0016756811000872 Published online by Cambridge University Press

The MGC is widely considered to have formed from the syntectonic emplacement of island arc magmas related to the initiation of a subduction zone beneath Connemara (Yardley & Senior, 1982; Dewey & Shackleton, 1984; Leake, 1989; Wellings, 1998) and Grampian orogenesis (Friedrich *et al*. 1999). The parental magmas for the MGC are suggested to have been hydrous island arc tholeiites (or boninites) rather than typical high-K or calc-alkaline island arc magmas (Leake, 1989). The field observations presented here, together with previous work (Ingold, 1937; Rothstein, 1957; Kanaris-Sotiriou & Angus, 1976; Bennett & Gibb, 1983; Wellings, 1997, 1998; Friedrich *et al*. 1999; O'Driscoll, 2005; O'Driscoll, Powell & Reavy, 2005) indicate that whilst the Dawros body is best interpreted as an open-system layered mafic intrusion, the Cr-spinel mineral chemistry bears strong similarities to ophiolitic Cr-spinel compositions. In particular, a strong Cr–Al trend (Fig. 5c) is observed, coupled with low TiO_2 and Al_2O_3 contents, although the high $Fe^{2+}/(Fe^{2+} + Mg)$ Cr-spinel values are more consistent with chromitites in layered mafic intrusions (Fig. 7). The very high Cr content of the Cr-spinel, together with low Al_2O_3 and low TiO_2 contents are indicative of crystallization from a parental magma that was generated through high degrees of partial melting of a mantle source that had probably already undergone a melting event (Zhou & Robinson, 1997; Rollinson, 2008; Uysal *et al*. 2009). The water-rich nature of the intrusions within the DCDC and related complexes, is emphasized by the presence of ubiquitous igneous hornblende and very calcic plagioclase ($An_{91.5}$ Currywongaun–Doughruagh Complex, Leake, 1958, 1964; Rothstein, 1957; Bremner & Leake, 1980), a typical feature of intrusions formed within supra-subduction zone tectonic settings (Pearce, Lippard & Roberts, 1984). These findings provide supporting evidence for the observations of previous workers that the mantle wedge beneath Connemara was undergoing fluid-enhanced melting in an island arc setting at the time of emplacement of the MGC and DCDC (Fig. 9a; Wellings, 1998; Friedrich *et al*. 1999; Zhou & Robinson, 1997; Kamenetsky, Crawford & Meffre, 2001; Rollinson, 2008; Uysal *et al*. 2009). Thus, a deeply sourced (Fig 9b), depleted island arc tholeiite or boninitic parental magma composition best explains the mineral chemical data, as also suggested by Leake (1989). This can be further constrained through calculation of the parental melt Al_2O_3 and TiO_2 content, as follows (after Maurel & Maurel, 1982; Page & Barnes, 2009):

$$(Al_2O_3 wt\%)_{spl} = 0.035(Al_2O_3 wt\%)^{2.42}_{melt}$$

$$\ln(TiO_2 wt\%)_{melt} = 0.82574 \times (\ln(TiO_2 wt\%)_{spl}) + 0.20203$$

which results in a parental melt Al_2O_3 content of 11.24–13.99 wt % (mean 11.86 wt %) and a TiO_2 content of 0.36–0.47 wt % (mean 0.39 wt %), which are both within the range of boninitic composition magmas (Al_2O_3 = 10.6–14.4 wt %; Wilson, 1989; TiO_2 = < 0.5 wt %; Sobolev & Danyushevsky, 1994; Fig 9c), further supporting the generation of the Dawros chromitites in a supra-subduction zone setting.

7. Conclusions

The Dawros chromitites exhibit unusual compositions for crystallization in a layered mafic intrusion (Barnes & Roeder, 2001). Their high Cr no. (0.50–0.87) combined with their low TiO_2 content (0.18–0.32 wt %) indicates that the chromitites probably formed in a mid-level magma chamber in a supra-subduction zone tectonic setting. Calculation of the parental melt Al_2O_3 and TiO_2 contents (~11.86 wt % and ~0.39 wt %, respectively) suggests that the Cr-spinel seams crystallized from boninitic magma, generated through high degrees of melting of an already depleted mantle source. The location of the chromitites immediately below a major lithological change from the harzburgite group upwards into the lherzolite group is suggestive of open-system magma chamber behaviour and that the chromitites potentially formed in response to new magma injection, as observed in other open-system layered mafic intrusions. Textural coarsening occurred within the chromitites as a primary magmatic (sub-solidus) effect during cooling and solidification of the Dawros Peridotite. Although high temperature regional metamorphism would have served to enhance this effect, petrographic evidence suggests that it is not required to produce the observed textures.

Acknowledgements. We would like to thank Tom Culligan (University College Dublin) for exceptional thin-sections and Andreas Kronz for his support with electron microprobe analyses at Universität Göttingen. Hugh Rollinson (University of Derby) is thanked for helpful discussion on classifying parental magma compositions. Brian McConnell and an anonymous reviewer are thanked for their constructive reviews, as is Phillip Leat for his thoughtful editorial support.

References

AHMED, A. H., ARAI, S., ADBEL-AZIZ, Y. M., IKENNE, M. & RAHIMI, A. 2009. Platinum-group elements distribution and spinel composition in podiform chromitites and associated rocks from the upper mantle section of the Neoproterozoic Bou Azzer ophiolite, Anti-Atlas, Morocco. *Journal of African Earth Sciences* **55**, 92–104.

BALLHAUS, C., BERRY, R. F. & GREEN, D. H. 1991. High pressure experimental calibration of the olivine-orthopyroxene-spinel oxygen geobarometer: implications for the oxidation state of the upper mantle. *Contributions to Mineralogy and Petrology* **101**, 27–40.

BALLHAUS, C. 1998. Origin of podiform chromite deposits by magma mingling. *Earth and Planetary Science Letters* **156**, 185–93.

BARNES, S. J. 1998. Chromite in komatiites, 1. Magmatic controls on crystallisation and composition. *Journal of Petrology* **39**, 1689–720.

BARNES, S. J. & ROEDER, P. L. 2001. The range of spinel compositions in terrestrial mafic and ultramafic rocks. *Journal of Petrology* **42**, 2279–302.

https://doi.org/10.1017/S0016756811000872 Published online by Cambridge University Press

BENNETT, M. C. & GIBB, F. G. F. 1983. Younging directions in the Dawros peridotite, Connemara. *Journal of the Geological Society, London* **140**, 63–73.

BONAVIA, F. F., DIELLA, V. & FERRARIO, A. 1993. Precambrian podiform chromites from Kenticha Hill, Southern Ethiopia. *Economic Geology* **88**, 108–202.

BOORMAN, S., BOUDREAU, A. & KRUGER, F. J. 2004. The Lower Zone–Critical Zone transition of the Bushveld Complex: a quantitative textural study. *Journal of Petrology* **45**, 1209–35.

BÜCHL, A., BRÜGMANN, G. & BATANOVA, V. G. 2004. Formation of podiform chromitite deposits: implications from PGE abundances and Os isotopic compositions of chromites from the Troodos complex, Cyprus. *Chemical Geology* **208**, 217–32.

BREMNER, D. L. & LEAKE, B. E. 1980. The geology of the Roundstone Ultrabasic Complex, Connemara. *Proceedings of the Royal Irish Academy* **80B**, 395–433.

DEWEY, J. F. & SHACKLETON, R. M. 1984. A model for the evolution of the Grampian tract in the early Caledonides and Appalachians. *Nature* **312**, 115–21.

DROOP, G. T. R. 1987. A general equation for estimating Fe^{3+} concentrations in ferromagnesian silicates and oxides from microprobe analyses, using stoichiometric criteria. *Mineralogical Magazine* **51**, 431–5.

FRIEDRICH, A. M., BOWRING, S. A., MARTIN, M. W. & HODGES, K. V. 1999. Short-lived continental magmatic arc at Connemara, western Irish Caledonides: implications for the age of the Grampian orogeny. *Geology* **27**, 27–30.

HIGGINS, M. D. 2000. Measurement of crystal size distributions. *American Mineralogist* **85**, 1105–16.

HIGGINS, M. D. 2006. *Quantitative Textural Measurements in Igneous and Metamorphic Petrology*. Cambridge: Cambridge University Press, 265 pp.

HIGGINS, M. D. 2009. *CSD Corrections version 1.3.9.1* [Digital Download]. http://depcom.uqac.ca/~mhiggins/csdcorrections.html.

HIGGINS, M. D. 2010. Textural coarsening in igneous rocks. *International Geology Review* **1**, 1–23.

HULBERT, L. J. & VON GRUENEWALDT, G. 1985. Textural and compositional features of chromite in the Lower and Critical Zones of the Bushveld Complex, South of Potgietersrus. *Economic Geology* **80**, 872–95.

INGOLD, L. M. 1937. The geology of the Currywongaun-Doughruagh area, Co. Galway. *Proceedings of the Royal Irish Academy* **B43**, 135–59.

IRVINE, T. N. 1965. Chromian spinel as a petrogenetic indicator: part 1. Theory. *Canadian Journal of Earth Sciences* **2**, 648–72.

IRVINE, T. N. 1967. Chromian spinel as a petrogenetic indicator: part 2. Petrologic applications. *Canadian Journal of Earth Sciences* **4**, 71–103.

IRVINE, T. N. 1977. Origin of chromite layers in the Muskox intrusion and other intrusion: a new interpretation. *Geology* **5**, 273–7.

KAMENETSKY, V. S., CRAWFORD, A. J. & MEFFRE, S. 2001. Factors controlling chemistry of magmatic spinel: an empirical study of associated olivine. *Journal of Petrology* **42**, 655–71.

KANARIS-SOTIRIOU, R. & ANGUS, N. S. 1976. The Currywongaun-Doughruah syntectonic intrusion, Connemara, Ireland. *Journal of the Geological Society, London* **132**, 485–508.

KELEMEN, P. B., WHITEHEAD, J. A., AHARONOV, E. & JORDAHL, K. A. 1995. Experiments on flow focusing in soluble porous media, with applications to melt extraction from the mantle. *Journal of Geophysical Research* **100**, 475–96.

KELEMEN, P. B., HIRTH, G., SHIMIZU, N., SPIEGELMAN, M. & DICK, H. J. B. 1997. A review of melt migration processes in the adiabatically upwelling mantle beneath oceanic spreading ridges. *Philosophical Transactions of the Royal Society of London* **A355**, 283–318.

LEAKE, B. E. 1958. The Cashel-Lough Wheelaun Intrusion, Co. Galway. *Proceedings of the Royal Irish Academy* **59B**, 155–203.

LEAKE, B. E. 1964. New light on the Dawros peridotite, Connemara, Ireland. *Geological Magazine* **101**, 63–75.

LEAKE, B. E. 1970. The fragmentation of the Connemara basic and ultrabasic intrusions. In *Mechanism of Igneous Intrusion* (eds G. Newall & N. Rast), pp 103–22. Liverpool: Seel House Press.

LEAKE, B. E. 1989. The metagabbros, orthogneisses and paragneisses of the Connemara complex, western Ireland. *Journal of the Geological Society, London* **146**, 575–96.

LEAKE, B. E. & TANNER, P. W. G. 1994. *The Geology of the Dalradian and Associated Rocks of the Connemara, Western Ireland: A report to accompany the 1:63360 geological map and cross-sections*. Dublin: Royal Irish Academy.

LORD, R. A., PRICHARD, H. M., SÁ, J. H. S. & NEARY, C. R. 2004. Chromite geochemistry and PGE fractionation in the Campo Formoso Complex and Ipueira-Medrado Sill, Bahia State, Brazil. *Economic Geology* **99**, 339–63.

MARCHESI, C., GONZÁLEZ-JIMÉNEZ, J. M, GERVILLA, F., GARRIDO, C. J., GRIFFIN, W. L., O'REILLY, S. Y., PROENZA, J. A. & PEARSON, N. J. 2011. In situ Re–Os isotopic analysis of platinum-group minerals from the Mayarí-Cristal ophiolitic massif (Mayarí-Baracoa Ophiolitic Belt, eastern Cuba): implications for the origin of Os-isotope heterogeneities in podiform chromitites. *Contributions to Mineralogy and Petrology* **161**, 977–90.

MARSH, B. D. 1998. On the interpretation of crystal size distributions in magmatic systems. *Journal of Petrology* **39**, 553–99.

MAUREL, C. & MAUREL, P. 1982. Etude experimentale de la distribution de l 'aluminium entre bain silicate basique et spinelle chromifere: implications petrogenetiques, teneur en chrome des spinelles. *Bulletin of Mineralogy* **105**, 97–202.

MELCHER, F., GRUM, W., SIMON, G., THALHAMMER, T. V. & STUMPEL, E. F. 1997. Petrogenesis of the ophiolitic giant chromite deposits of Kempirsai, Kazakhstan: a study of solid and fluid inclusions in chromite. *Journal of Petrology* **38**, 1419–58.

MONDAL, S. K. & MATHEZ, E. A. 2007. Origin of the UG2 chromitite layer, Bushveld Complex. *Journal of Petrology* **48**, 495–519.

NALDRETT, A. J., KINNAIRD, J., WILSON, A., YUDOSKAYA, M., MCQUADE, S., CHUNNETT, G. & STANLEY, C. 2009. Chromitite composition and PGE content of the Bushveld chromitites: Part 1 – the Lower and Middle Groups. *Applied Earth Sciences (Transactions of the Institution of Mining and Metallurgy, Section B)* **118**, 131–61.

O'DRISCOLL, B. 2005. Textural equilibrium in magmatic layers of the Lough Fee ultramafic intrusion, NW Connemara, Ireland: implications for adcumulus mineral growth. *Irish Journal of Earth Sciences* **23**, 39–45.

O'DRISCOLL, B., DONALDSON, C. H., DALY, J. S. & EMELEUS, C. H. 2009. The roles of melt infiltration and cumulate assimilation in the formation of anorthosite

and a Cr-spinel seam in the Rum Eastern Layered Intrusion, NW Scotland. *Lithos* **111**, 6–20.

O'Driscoll, B., Emeleus, C. H., Donaldson, C. H. & Daly, J. S. 2010. Cr-spinel seam petrogenesis in the Rum Layered Suite, NW Scotland: cumulate assimilation and *in situ* crystallization in a deforming crystal mush. *Journal of Petrology* **51**, 1171–201.

O'Driscoll, B. & Petronis, M. S. 2009. Oxide mineral formation during the serpentinization of a Cr-spinel seam: insights from rock magnetic experiments. *Geochemistry, Geophysics, Geosystems* **10**, Q01008, doi:10.1029/2008GC002274.

O'Driscoll, B., Powell, D. G. R. & Reavy, R. J. 2005. Constraints on the development of magmatic layering in a syntectonic mafic-ultramafic suite, NW Connemara, Ireland. *Scottish Journal of Geology* **41**, 119–28.

Page, P. & Barnes, S. J. 2009. Using trace elements in chromites to constrain the origin of podiform chromitites in the Thetford Mines Ophiolite, Québec, Canada. *Economic Geology* **104**, 997–1018.

Pearce, J. A., Lippard, S. J. & Roberts, S. 1984. Characteristics and tectonic significance of supra-subduction zone ophiolites. In *Marginal Basin Geology: Volcanic and associated sedimentary and tectonic processes in modern and ancient marginal basins* (eds B. P. Kokelaar & M. F. Howells), pp. 77–94. Geological Society of London, Special Publication no. 16.

Quintiliani, M., Andreozzi, G. B. & Graziani, G. 2006. Fe^{2+} and Fe^{3+} quantification by different approaches and f_{O2} estimation for Albanian Cr-spinels. *American Mineralogist* **91**, 907–16.

Rollinson, H. 2008. The geochemistry of mantle chromitites from the northern part of the Oman ophiolite: inferred parental melt compositions. *Contributions to Mineralogy and Petrology* **156**, 273–88.

Rollinson, H., Appel, P. W. U. & Frei, R. 2002. A metamorphosed Early Archean chromitite from West Greenland: implications for the genesis of Archean anorthositic chromitites. *Journal of Petrology* **43**, 2143–70.

Rothstein, A. T. V. 1957. The Dawros peridotite, Connemara, Eire. *Quarterly Journal of the Geological Society of London* **113**, 599–602.

Rothstein, A. T. V. 1972. Spinels from the Dawros Peridotite, Connemara, Ireland. *Mineralogical Magazine* **38**, 957–60.

Sobolev, A. V. & Danyushevsky, L. V. 1994. Petrology and geochemistry of boninites from the north termination of the Tonga Trench: constraints on the generation conditions of primary high-Ca boninite magmas. *Journal of Petrology* **35**, 1183–211.

Tanner, P. W. G. & Shackleton, R. M. 1979. Structure and stratigraphy of the Dalradian rocks of the Beannabeola area, Connemara, Eire. In *The Caledonides of the British Isles Reviewed* (eds A. L. Harris, C. H. Holland & B. E. Leake), pp 243–56. Geological Society of London, Special Publication no. 8.

Uysal, I., Tarkian, M., Sadiklar, M. B., Zaccarini, F., Meisel, T., Garuti, G. & Heidrich, S. 2009. Petrology of Al- and Cr-rich ophiolitic chromitites from the Muğla, SW Turkey: implications from composition of chromite, solid inclusions of platinum-group mineral, silicate, and base-metal mineral, and Os-isotope geochemistry. *Contributions to Mineralogy and Petrology* **158**, 659–74.

Waters, C. & Boudreau, A. E. 1996. A re-evaluation of crystal-size distributions in chromite cumulates. *American Mineralogist* **81**, 1452–9.

Wellings, S. A. 1997. Emplacement of mafic intrusions, north-west Connemara: constraints from petrology and structures. *Irish Journal of Earth Sciences* **16**, 71–84.

Wellings, S. A. 1998. Timing of deformation associated with the syn-tectonic Dawros-Currywongaun-Doughruah Complex, NW Connemara, western Ireland. *Journal of the Geological Society, London* **155**, 25–37.

Wilson, M. 1989. *Igneous Petrogenesis: A global tectonic approach*, 1st ed. London: Chapman & Hall, 466 pp.

Yardley, B. F. & Senior, A. 1982. Basic magmatism in Connemara, Ireland: evidence for a volcanic arc? *Journal of the Geological Society, London* **139**, 67–70.

Zhou, M.-F., Reid, M. S., Keays, R. R. & Kerrich, R. W. 1998. Controls on platinum-group elemental distributions of podiform chromitites: a case study of high-Cr and high-Al chromitites from Chinese orogenic belts. *Geochimica et Cosmochimica Acta* **62**, 677–88.

Zhou, M.-F. & Robinson, P. T. 1997. Origin and tectonic environment of podiform chromite deposits. *Economic Geology* **92**, 259–62.

Zhou, M.-F., Robinson, P. T., Malpas, J., Aitchison, J., Sun, M., Bai, W.-J., Hu, X.-F. & Yang, J.-S. 2001. Melt/mantle interaction and melt evolution in the Sartohay high-Al chromite deposits of the Dalabute ophiolite, NW China. *Journal of Asian Earth Sciences* **19**, 517–34.

Zhou, M.-F., Robinson, P. T., Malpas, J. & Li, Z. 1996. Podiform chromitites in the Luobusa Ophiolite (Southern Tibet): implications for melt-rock interaction and chromite segregation in the upper mantle. *Journal of Petrology* **37**, 3–21.